mg and the ketone amount was varied between 0.5 and 20 mg.

B. Zeolite–Hexane Slurry. Known amounts of guest ketones and the activated zeolites were stirred together in 5 mL of hexane for about 2 h. In a typical preparation, 200 mg of the zeolite and 5 mg of ketone were taken in 5 mL of the solvent. At the end of 2 h, the hexane layer was analyzed by GC for the presence of the ketone in the hexane portion. In no case did we find any guest in the hexane layer, indicating that all the initial ketone had been adsorbed into the zeolite.

Photophysical Studies. Diffuse reflectance spectra of the zeolite solid samples were measured in 2-mm-path-length quartz cells using a Varian 2400 spectrometer equipped with either an integrating sphere (Varian) or a "Praying Mantis" all-reflective light collection system (Harrick Scientific), in both cases using barium sulfate (Kodak, white reflectance standard) as the reference. Sample packing densities were not determined nor were they specifically controlled. Spectra were recorded between 220 and 500 nm. For comparison, spectra of the empty zeolites were also recorded. Data were recorded digitally, and appropriate background corrections were carried out using the computer program SpectraCalc (Galactic Industries).

Emission spectra were recorded at room temperature and at 77 K in Supracil quartz EPR tubes under degassed conditions with a Spex Fluorolog 212 spectrofluorimeter.

The experimental setup for diffuse reflectance laser flash photolysis measurements has been described elsewhere.[44] For these experiments, the fourth harmonic (266 nm, 10-ns pulses, ≤25 mJ/pulse) from a Lumonics HY-750 Nd:YAG laser was used for sample excitation. The samples were contained in 3 × 7 mm^2 quartz cuvettes and were deaerated by purging for at least 30 min with oxygen-free nitrogen. During the laser experiments the sample was either moved or shaken to ensure that a fresh sample surface was used for each laser shot.

Photolysis Studies. A. Dry Samples. Samples containing 125 mg of the complex were degassed in Pyrex cells and irradiated with 450-W mercury lamps. Irradiation cells were rotated periodically to provide uniform exposure. Generally about 15% conversion was obtained in about 2 h of irradiation. After photolysis, products were extracted by stirring the samples in ether (20 mL) for about 6 h. In some cases the zeolite was dissolved with concentrated HCl and extracted with ether. Control experiments established that the products are stable to the acid extraction conditions.

B. Zeolite–Hexane Slurry. A guest–zeolite–solvent slurry in a Pyrex test tube was purged with helium (making sure no evaporation of hexane occurred) for about 10 min and sealed. The above slurry was magnetically stirred and irradiated with 450-W mercury lamps with Pyrex filters for about 30 min. The hexane (or pentane) solvent was decanted and analyzed by GC. Neither starting reactants nor products were found in the supernatant solvent. Products and reactants were extracted from the zeolites by stirring them with diethyl ether (10 mL) for about 10 h. The ether extract was analyzed by GC as above.

Products from both dry zeolites and hexane slurries were analyzed by GC (Hewlett Packard Model 5890, SE-30 capillary column) and peaks were integrated with a Hewlett Packard integrator Model 3393A. The temperature of the analysis was between 80 and 250 °C depending on the ketone. The flame-ionization detector was not calibrated for differences in detector response to the various products and starting ketone. The elution order was as follows: solvent, acetophenone, type II olefin, *cis*-cyclobutanol, *trans*-cyclobutanol, and starting ketone. All peaks were identified by coinjection with authentic samples. *cis*- and *trans*-cyclobutanols were obtained by large-scale solution irradiation (2 × 50 mg/25 mL of benzene) and isolation by silica gel flash chromatography. These were characterized by comparison of their IR, NMR, and mass spectra with the literature reports.[25,30,41] It is to be noted that the *trans*-cyclobutanol elutes before the cis isomer during the silica gel flash chromatography.

Acknowledgment. It is a pleasure to thank D. Sanderson and P. Hollins for able technical assistance and Professors R. G. Weiss and P. Wagner for valuable discussions.

Registry No. 1a, 495-40-9; **1b**, 1009-14-9; **1c**, 1674-37-9; **1d**, 1674-38-0; **1e**, 4497-05-6; **1f**, 6786-36-3; AcPh, 98-86-2; Li, 7439-93-2; Na, 7440-23-5; K, 7440-09-7; Rb, 7440-17-7; Cs, 7440-46-2; $CH_3(CH_2)_4CH_3$, 110-54-3; 1-phenylcyclobutanol, 935-64-8; 2-methyl-1-phenylcyclobutanol, 82245-43-0; *cis*-2-butyl-1-phenylcyclobutanol, 95605-57-5; *trans*-2-butyl-1-phenylcyclobutanol, 95605-56-4; *cis*-2-octyl-1-phenylcyclobutanol, 126583-83-3; *trans*-2-octyl-1-phenylcyclobutanol, 126583-82-2; *cis*-2-decyl-1-phenylcyclobutanol, 126583-85-5; *trans*-2-decyl-1-phenylcyclobutanol, 126583-84-4; *cis*-1-phenyl-2-tetradecylcyclobutanol, 126583-87-7; *trans*-1-phenyl-2-tetradecylcyclobutanol, 126583-86-6.

(44) Kazanis, S.; Azarani, A.; Johnston, L. J. *J. Am. Chem. Soc.* **1991**, *95*, 4430.

Heavy-Atom-Induced Phosphorescence of Aromatics and Olefins Included within Zeolites

V. Ramamurthy,* J. V Caspar, D. F. Eaton, Erica W. Kuo, and D. R. Corbin

Contribution No. 6068 from Central Research and Development, Experimental Station, The Du Pont Company, Wilmington, Delaware 19880-0328. *Received December 2, 1991*

Abstract: Photophysical properties of naphthalene and other aromatic guest molecules included in X-type faujasite zeolites (M^+ X, M = Li, Na, K, Rb, Cs, Tl) have been investigated. As expected for an external heavy atom perturbed excited state, both singlet and triplet excited state lifetimes and emission efficiencies depend upon the identity and accessibility of the cation present within the zeolite supercage. The large magnitude of the external-heavy-atom perturbation is not unique to the X-type faujasites; similar effects for organic guests included in Y-type faujasites, in pentasils (ZSM-5 and ZSM-11), and in other zeolites (mordenite, β, L, and Ω) have been demonstrated. The power of the heavy-atom-cation effect in zeolites has been demonstrated by recording phosphorescence data from several olefins whose phosphorescence data has not been recorded previously. The heavy atom cation induced phosphorescence technique has been utilized to understand basic features of interaction between the zeolite and guest aromatic molecules.

Introduction

Studies utilizing a number of organized assemblies and surfaces to orient molecules have paved the way to an intriguing number of possibilities by which photochemical and photophysical properties of molecules can be modified.[1] In this context, the internal surfaces of zeolites have attracted recent attention.[2] Zeolites may be regarded as open structures of silica in which aluminum has been substituted into a number of the tetrahedral sites.[3] The

(1) Kalyanasundaram, K. *Photochemistry in Microheterogeneous Systems*; Academic Press: New York, 1987. Ramamurthy, V., Ed. *Photochemistry in Organized and Constrained Media*; VCH: New York, 1991.

(2) Turro, N. J. *Pure Appl. Chem.* **1986**, *58*, 1219. Turro, N. J. In *Molecular Dynamics in Restricted Geometries*; Klafter, J., Drake, J. M., Eds.; John Wiley: New York, 1989; p 387. Turro, N. J.; Garcia-Garibay, M. In *Photochemistry in Organized and Constrained Media*; Ramamurthy, V., Ed.; VCH: New York, 1991; p 1. Ramamurthy, V. In *Photochemistry in Organized and Constrained Media*; Ramamurthy, V., Ed.; VCH: New York, 1991; p 429. Kelly, G. K.; Willsher, C. J.; Wilkinson, F.; Netto-Ferreira, J. C.; Olea, A.; Weir, D.; Johnston, L.; Scaiano, J. C. *Can. J. Chem.* **1990**, *68*, 812 and other papers in the series. Sankaraman, S.; Yoon, K. B.; Kochi, J. K. *J. Am. Chem. Soc.* **1991**, *113*, 1419 and other papers in the series.

0002-7863/92/1514-3882$03.00/0

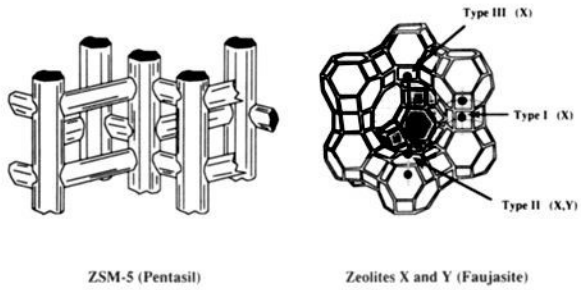

Figure 1. Structures of zeolites: ZSM-5 and faujasites (X and Y). Position of cations in X and Y zeolites shown as type I, II, and III.

frameworks thus obtained contain pores, channels, and cages. The substitution of trivalent aluminum ions for a fraction (≤ 0.5) of the tetravalent silicon ions at lattice positions results in a network that bears a net negative charge, which must be compensated by counterions. The latter are mobile and may occupy various exchange sites depending upon their radius, charge, and degree of hydration. They can be replaced, to varying degrees, by exchange with other cations. These cations are expected to contribute significantly to the nature of the local microenvironment within the cage, channel, and pore. Spin-state interconversion (singlet–triplet intersystem crossing) of excited guests is one physical process which might be anticipated to be modified by cation type. In this paper we demonstrate that one can control the extent of the excited singlet and triplet interconversion of the excited guest molecule within a cage, channel, or pore by controlling interactions of guests with the exchanged cation and establish that the heavy atom cation exchanged zeolites are a novel new medium capable of yielding dramatic heavy-atom perturbation of organic chromophores.[4]

A brief description of the structure of the zeolites used in this study is appropriate. The topological structure of X- and Y-type zeolites consists of an interconnected three-dimensional network of relatively large spherical cavities, termed supercages (diameter about 13 Å, Figure 1). Each supercage is connected tetrahedrally to four other supercages through 8-Å windows or pores. The interiors of zeolites X and Y also contain, in addition to supercages, smaller sodalite cages. The windows to the sodalite cages are too small to allow organic molecules access to these cages. Charge-compensating cations present in the internal structure are known to occupy three different positions (Figure 1) in zeolites X and Y. Only cations of sites II and III are expected to be readily accessible to the adsorbed organic molecule. Among the medium-pore-sized zeolites, perhaps the most studied are the pentasil zeolites, ZSM-5 and ZSM-11 (Figure 1). These zeolites also have three-dimensional pore structures; a major difference between the pentasil pore structures and those of the faujasites described above is the fact that the pentasil pores do not link cage structures as such. Instead, the pentasils are composed of two intersecting channel systems. For ZSM-5, one system consists of straight channels with a free diameter of about 5.4 × 5.6 Å, and the other consists of sinusoidal channels with a free diameter of about 5.1 × 5.5 Å. For ZSM-11, both are straight channels with dimensions of about 5.3 × 5.4 Å. Other zeolites of interest for photochemical and photophysical studies include L, mordenite, Ω, and β.

(3) Meier, W. M.; Olson, D. H. *Atlas of Zeolite Structure Types*, 2nd revised ed.; Butterworths: Cambridge, 1987. Breck, D. W. *Zeolite Molecular Sieves: Structure, Chemistry, and Use*; John Wiley and Sons: New York, 1974. Dyer, A. *An Introduction to Zeolite Molecular Sieves*; John Wiley and Sons: Bath, 1988. *Introduction to Zeolite Science and Practice*; van Bekkum, H., Flanigen, E. M., Jansen, J. C., Eds.; Elsevier: Amsterdam, 1991.

(4) For an early report of heavy-atom effects in zeolites: Bobonich, F. M. *Zh. Prikl. Spektrosk.* **1978**, *28*, 145. In one of the recent studies, quenching of pyrene singlet in M^+ X zeolites (M = Li, Na, K, and Tl) have been attributed to an electron-transfer process between the guest and the cation: Iu, K. K.; Thomas, J. K. *J. Phys. Chem.* **1991**, *95*, 506. Iu, K. K.; Thomas, J. K. *Langmuir* **1990**, *6*, 471. For a preliminary communication of our results, see: Ramamurthy, V.; Caspar, J. V.; Corbin, D. R.; Eaton, D. F. *J. Photochem. Photobiol., A* **1989**, *50*, 157.

Results and Discussion

In this study we have utilized several aromatics (naphthalene, anthracene, phenanthrene, chrysene, pyrene, acenaphthene, and hexahydropyrene) to explore the heavy-atom-cation effect in zeolites. The generality with respect to zeolite has been established by utilizing several types of zeolites (X, Y, ZSM-5, ZSM-11, L, mordenite, Ω and β). Cations exchanged were lithium, sodium, potassium, rubidium, cesium, and thallium. A detailed mechanistic investigation has been carried out with naphthalene in M^+ X and M^+ Y zeolites, and the conclusions drawn from this system are extended to other aromatics and zeolites. The power of the heavy-atom-cation effect in zeolites has been demonstrated by recording phosphorescence data from several olefins whose phosphorescence data has not been recorded before. Finally, we have utilized this technique to understand some basic features of the interaction between the zeolite and the guest aromatic molecules. Results are discussed under three subsections below.

In order to establish a fairly routine and simple procedure for the preparation of zeolite–guest complexes, we prepared the naphthalene–Na X complex by four independent methods and recorded the diffuse reflectance and emission spectra and measured the singlet lifetimes under degassed and oxygenated conditions. The four methods are as follows: (1) Na X was calcined at 500 °C on a vacuum line at 10^{-4} mm. The dry zeolite was taken into a drybox under sealed conditions, and the complex was prepared by grinding the guest naphthalene and Na X together. Sample preparation for recording spectra, etc., was performed within the drybox. (2) The dry complex prepared above was exposed to atmospheric moisture by keeping it on the pan of a Mettler balance. The sample gained weight to the extent of ~22% by absorbing moisture. The complex thus treated is believed to be wet and to contain both naphthalene and water within the supercage. (3) Na X dried at 500 °C in a furnace open to air was transferred at ~100 °C to a hexane or trimethylpentane solution containing naphthalene. The solution was stirred for about 6 h. The complex was collected by filtration and dried on a vacuum line at 10^{-5} mm. (4) Furnace-dried Na X was exposed to atmospheric moisture by being kept on the pan of a Mettler balance. It gained weight (~23%), indicating that it is clearly wet and the cages are filled with water. This wet zeolite was used for complex preparation by solution (hexane) and solid (grinding) methods. In all cases except the last, where wet Na X was used, inclusion of naphthalene occurred. In the last case, the diffuse reflectance spectra indicated that only very little naphthalene is adsorbed. However, the amount adsorbed was sufficient to record the emission spectra and monitor the S_1 lifetime. Little difference in lifetime was noticed between the sample prepared within the drybox and the one prepared by the solution method ($\tau_{s(1)}$ 45.2 and 49.1 ns, respectively). Both samples are quenched equally efficiently by oxygen (τ_s 16.9 and 17.6 ns, respectively). However, when the samples were wetted as in methods 2 and 4 above, they were inefficiently quenched by oxygen (τ_s for samples from method 2, degassed 35.4 and oxygenated 31.6 ns; τ_s for samples from method 4, degassed 44.8 and oxygenated 37.9 ns). Inefficient quenching indicates that the oxygen diffusion within the internal structure of the zeolite is prevented by water molecules. On the basis of these experiments, we decided to utilize the solution method, a method much simpler than the drybox procedure, for all of our complexation. Sample handling under laboratory conditions is often facilitated by dry weather. Photophysical measurements, in general, were made on solvent-free dry complexes under aerated conditions. Occasionally, samples in sealed ESR tubes were used for emission and lifetime measurements. Guest loading was about 0.1 molecule/supercage in the case of X and Y zeolites, i.e., an occupancy number of about 0.1 (occupancy number is defined as the number of guest molecules to the number of available supercages and is represented by $\langle S \rangle$). This roughly corresponds to about 0.01 mg of guest/250 mg of dry zeolite. It should be noted that in order to maintain the same loading level (supercage/guest ratio) with various cation-exchanged zeolites, one has to take increasing amounts of zeolites with increasing atomic weight of the cation. Inclusion of guests

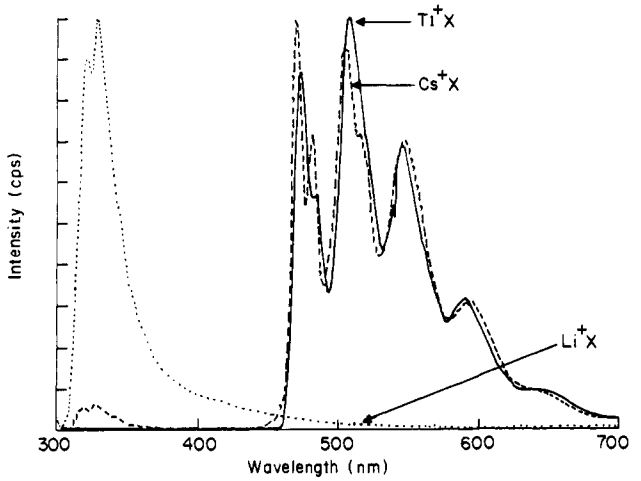

Figure 2. Emission spectra at 77 K of naphthalene included in Li X, Cs X, and Tl X (excitation λ: 285 nm). Note that the ratio of phosphorescence to fluorescence changes with the cation but the ratio change is independent of the excitation wavelength.

Table I. Photophysical Parameters for Naphthalene Included in Zeolites[a]

zeolite host	triplet lifetime[b] (s)	singlet lifetime[c] (ns)	P/F[d]
Li X	-	33.0	1.0×10^{-4}
Na X	-	35.4	7.3×10^{-2}
K X	1.72	19.4	0.16
Rb X	0.72	2.22	8.1
Cs X	0.20	0.23 (87%), 1.87 (13%)	45
Tl X	0.0012	-	only P
Li Y	-	31.8	1.2×10^{-3}
Na Y	-	25.1	1.0×10^{-3}
K Y	-	13.8	0.1
Rb Y	-	3.8	9.0
Cs Y	-	0.7	60

[a] Loading level in all cases corresponds to about 0.01. [b] The lifetime measured at 77 K. [c] The lifetime measured at 298 K. [d] Phosphorescence to fluorescence intensity ratio estimated at 77 K; the number is independent of the wavelength of excitation.

within zeolites was confirmed by diffuse reflectance spectra of the complexes, none of which are reproduced here. Also, GC analysis of the supernatant solvent from the complexation process revealed that no guest remained in the solvent.

1. Aromatics. Naphthalene exhibits intense fluorescence in solution at room temperature and intense fluorescence plus weak phosphorescence in glassy matrices at 77 K. We find that naphthalene, when included into X and Y zeolites (M^+ X and M^+ Y, M = Li, Na, K, Rb, Cs, and Tl), shows unique emission behavior which depends on the nature of the metal cations present within the zeolite structure. Emission of naphthalene in Li X both at room temperature and at 77 K consists only of fluorescence (Figure 2). We observed dramatic differences in the emission of naphthalene in Tl X; phosphorescence is the only emission both at room temperature and at 77 K (Figure 2). The naphthalene phosphorescence to fluorescence intensity ratio (P/F) is seen to increase (Table I), although not linearly, as lighter cations are replaced with heavier ones in both the X- and Y-type zeolites (Table I; Li < Na < K < Rb < Cs < Tl).

Table I lists excited singlet lifetimes (at room temperature) and triplet lifetimes (at 77 K) of naphthalene included within various cation-exchanged zeolites. It is clear that both these lifetimes are cation dependent. A word about lifetimes is in order.[5] At low temperatures where the phosphorescence yield is independent of

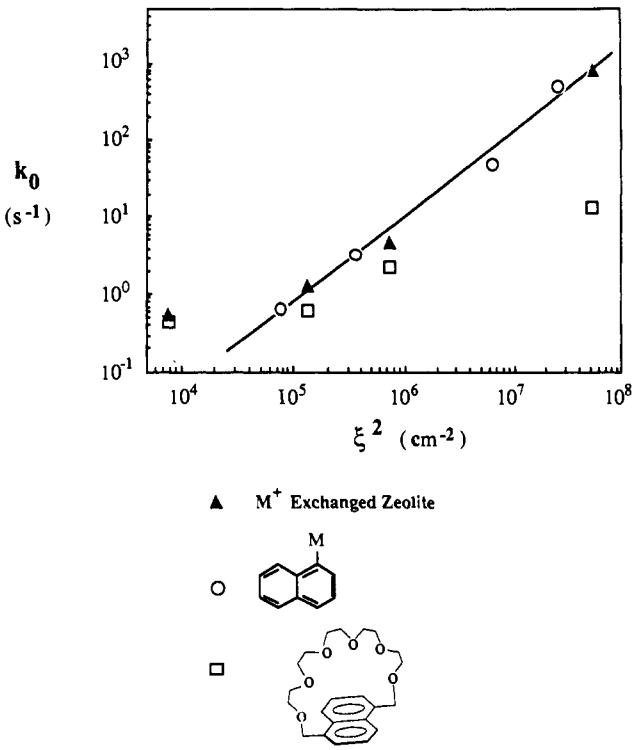

Figure 3. A linear relationship between the triplet decay of naphthalene in M X zeolites and the spin–orbit coupling parameter of the cation. Similar relationships for 1-halonaphthalenes and cation-complexed 1,5-naphtho-22-crown-6 are also shown.

Chart I

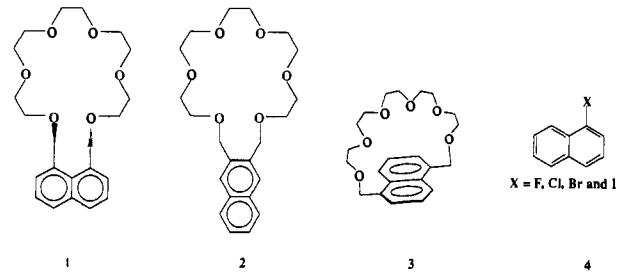

temperature (less than ca. 150 K), the triplet lifetime of naphthalene can be represented by a single first-order decay for all of the zeolite samples investigated here. However, at higher temperatures, lifetimes are composed of two independent first-order decay pathways. The numbers reported in Table I are in the region where the triplet lifetime is single exponential and is independent of temperature. Singlet lifetimes were measured only at room temperature. Generally, a good fit can be obtained with a single exponential. Only in the case of Cs X was a double exponential fit needed to obtain acceptable statistical parameters. All lifetime measurements were made only for one loading level (occupancy number, $\langle S \rangle$, 0.01).

The trend in lifetimes observed for naphthalene within zeolites is similar to that reported by Sousa and co-workers for naphthalene-derived crown ether systems (**1–3**, Chart I) perturbed by alkali metal cations.[6] We show below that the heavy-cation effect Sousa and co-workers observed is responsible for the enhanced phosphorescence and decreased singlet and triplet lifetimes for naphthalene within potassium-, rubidium-, cesium-, and thallium-cation-exchanged faujasites. It is well-known that the effect of external-heavy-atom perturbation scales with the square of the perturber's spin–orbit coupling constant, ξ^2, and that a log–log plot of τ_T^{-1} vs ξ^2 should be linear with a maximum predicted slope

(5) In general, lifetimes of excited species on surfaces have been found to follow multiexponential decay: Bohne, C.; Redmond, R. W.; Scaiano, J. C. In *Photochemistry in Organized and Constrained Media*; Ramamurthy, V., Ed.; VCH: New York, 1991; p 79. Ware, W. R. In *Photochemistry in Organized and Constrained Media*; Ramamurthy, V., Ed.; VCH: New York, 1991; p 563.

(6) Larson, J. M.; Sousa, L. R. *J. Am. Chem. Soc.* **1978**, *100*, 1942. Ghosh, S.; Petrin, M.; Maki, A. H.; Sousa, L. R. *J. Chem. Phys.* **1987**, *87*, 4315. Ghosh, S.; Petrin, M.; Maki, A. H.; Sousa, L. R. *J. Chem. Phys.* **1988**, *88*, 2913.

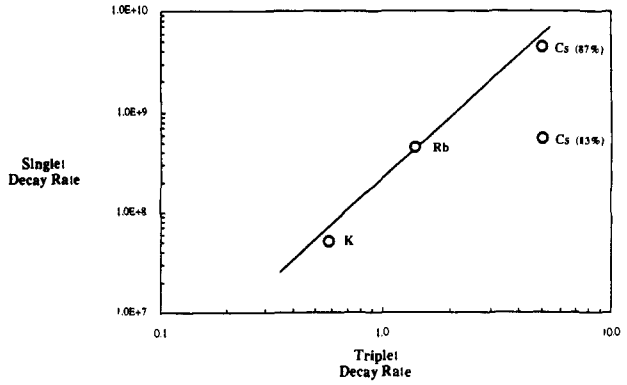

Figure 4. Linear relationship between singlet and triplet decay of naphthalene in M X zeolites. Both singlet and triplet decays are influenced by the cation.

of unity.[7] As shown in Figure 3, we observe the expected dependence. For comparison we have also provided in Figure 3 the linear relationship observed in two systems, namely, 1,5-naphtho-22-crown-6 (**3**) and 1-halonaphthalenes (**4**), where the external- and internal-heavy-atom effects, respectively, are presumed to operate. The magnitude of the heavy-atom effect we observe in zeolites is significantly larger than that observed for the 1,5-naphtho-22-crown-6 (**3**) exchanged with heavy-atom cations, where the cation is rigidly held over the naphthalene π-face. In fact the zeolite samples show heavy-atom effects nearly as large as for a series of 1-halonaphthalenes (**4**) where the perturbers are covalently attached to the chromophore.[7] We attribute this result both to the close approach between naphthalene and the heavy atom, which is enforced by the zeolite supercage, and to the presence of more than one heavy-atom cation per supercage, which leads to highly effective concentrations of the heavy-atom cation in the vicinity of the naphthalene. It is important to note that the τ_T^{-1} that we measure at 77 K is the sum of radiative and nonradiative terms which cannot be separated in the absence of absolute phosphorescence quantum yield measurements. External-heavy-atom perturbation is expected to enhance radiative rates more than nonradiative,[8] and hence variations in τ_T^{-1} between different heavy-atom cations should primarily reflect variations in radiative rate k_r from T_1 to S_0, as long as the phosphorescence yields are significantly less than unity.

For the cations we studied (K^+, Rb^+, Cs^+, Tl^+), the relative emission quantum yield of the naphthalene singlet state is essentially temperature independent from 77 to 295 K, indicating that $S_1 \rightarrow S_0$ radiative and nonradiative rates and $S_1 \rightarrow T_1$ intersystem crossing rates are unaffected by temperature and that there are no thermally activated processes leading to population of the S_1 excited state from naphthalene triplet states. These observations also argue against any diffusional triplet–triplet annihilation contribution to naphthalene triplet decay in this temperature regime. While we have not measured absolute efficiencies, it is clear that the relative $S_1 \rightarrow S_0$ emission efficiencies decrease as the cation mass increases in the series $Li^+ \approx Na^+ \approx K^+ < Rb^+ < Cs^+ \ll Tl^+$. As the heavy-atom effect is not expected to significantly affect the radiative and radiationless decay from S_1 to S_0, we interpret the decrease in singlet emission efficiency and lifetime to an increase in the rate of intersystem crossing from S_1 to T_1 due to external-heavy-atom perturbation. If the heavy-cation effect is indeed responsible for the variations in singlet and triplet lifetimes, one would expect a linear relationship between singlet and triplet decays with cation variation. Indeed this is observed as shown in Figure 4. The slope of the line suggests that the singlet decay is enhanced more than the triplet, consistent

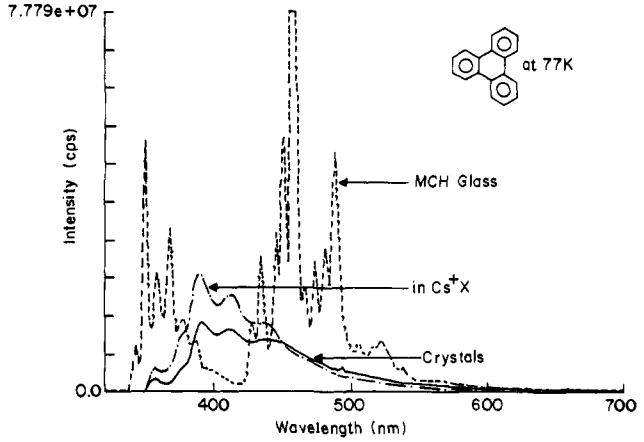

Figure 5. Emission spectra at 77 K of triphenylene as microcrystals, in MCH glass, and adsorbed on Cs X zeolites (excitation λ: 280 nm). Notice the similarity between spectra of triphenylene as microcrystals and on Cs X. Only in MCH glass is distinct phosphorescence seen.

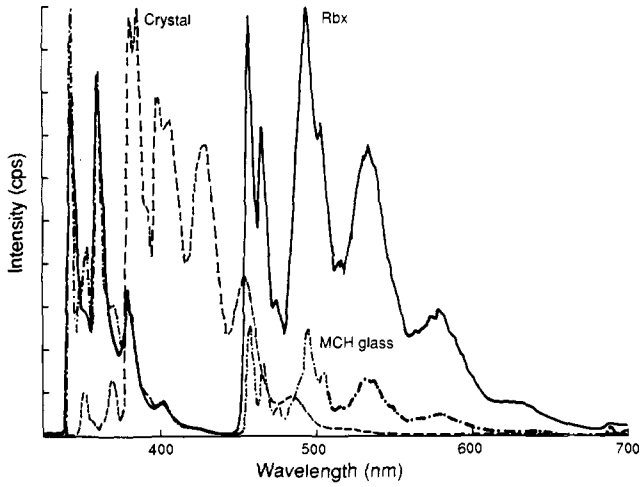

Figure 6. Emission spectra at 77 K of phenanthrene as microcrystals (– – –), in MCH glass (–·–·–), and included in Rb X zeolites (excitation λ: 295 nm). Notice the similarity between spectra in MCH glass and in Rb X.

with the smaller energy gap between S_1 and T_1 as compared to T_1 and S_0.

It is clear from the above correlations that the heavy-cation effect is responsible for the variations in photophysical properties observed in this study. It has been demonstrated that the external-heavy-atom effect is operative only at close distances.[9] The following results suggest that only when the cation and the guest molecules are contained within the same supercage is the heavy-atom-induced phosphorescence observed. First, larger aromatics such as triphenylene and coronene do not exhibit enhanced phosphorescence in the presence of rubidium- or cesium-exchanged faujasites. In Figure 5 we provide the emission spectra of triphenylene in methylcyclohexane (MCH) glass, in Cs X, and as microcrystals. The spectra of triphenylene in Cs X is the same as that of triphenylene as microcrystals, suggesting that triphenylene did not enter the pores of the faujasites. This becomes clear when the emission spectra of phenanthrene under the above conditions are considered (Figure 6). In this case, spectra in methylcyclohexane glass and in Rb X bear similarity, and they are distinctly different from that of phenanthrene as microcrystals. This suggests that phenanthrene molecules are not aggregated and are possibly isolated by supercages of zeolite. Further, the heavy-atom-cation effect is reflected by the enhanced phosphorescence. We conclude that large aromatics such as tri-

(7) Kasha, M. *J. Chem. Phys.* **1952**, *20*, 71. McClure, D. S. *J. Chem. Phys.* **1949**, *17*, 905.

(8) McGlynn, S. P.; Reynolds, M. J.; Daigre, G. W.; Christodoyleas, N. D. *J. Phys. Chem.* **1962**, *66*, 2499. McGlynn, S. P.; Sunseri, R.; Christodouleas, N. *J. Chem. Phys.* **1962**, *37*, 1818. McGlynn, S. P.; Azumi, T.; Kinoshita, M. *Molecular Spectroscopy of the Triplet State*; Prentice-Hall: Englewood Cliffs, NJ, 1969.

(9) Chandra, A. K.; Turro, N. J.; Lyons, A. L.; Stone, P. *J. Am. Chem. Soc.* **1978**, *100*, 4964. Turro, N. J. *Modern Molecular Photochemistry*; Benjamin Cummins: Menlo Park, 1978; pp 117–130, 185–193.

Table II. Singlet Lifetime[a] and Phosphorescence to Fluorescence Emission Intensity Ratio (P/F)[b] for Aromatics Included in M^+ X and M^+ Y Zeolites[a-c]

	phenanthrene		pyrene		hexahydropyrene		acenaphthene		chrysene	
zeolite	$\tau_{s(1)}$, ns	P/F	$\tau_{s(1)}$, ns	P/F	$\tau_{s(1)}$, ns	P/F	$\tau_{s(1)}$, ns	P/F	$\tau_{s(1)}$, ns	P/F
Li X	31.2	0.11	146.4	0.001	15.3	0.14	-	0.01	32.9	0.05
Na X	36.6	0.28	187.4	0.001	12.7	0.28	11.7	0.3	27.1	0.15
K X	27.5	0.40	161.4	0.03	18.2	0.38	13.1	0.7	20.3	1.1
Rb X	3.6	3.7	63.9	0.07	3.4	0.71	2.7	1.7	5.4	5.3
Cs X	0.3	74	5.7	0.21	1.1	4.0	1.0	10.3	4.1	60.7

[a] Loading level in all cases corresponds to about 0.01. [b] The lifetime measured at 298 K. [c] Phosphorescence to fluorescence intensity ratio estimated at 77 K; the number is independent of the wavelength of excitation.

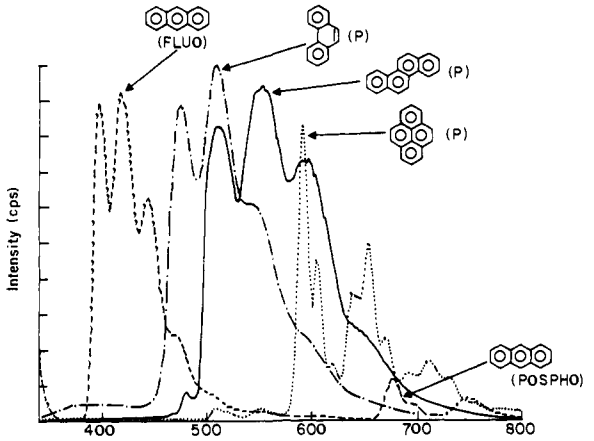

Figure 7. Emission spectra at 298 K of anthracene (excitation λ: 340 nm), phenanthrene (excitation λ: 295 nm), chrysene (excitation λ: 320 nm), and pyrene (excitation λ: 340 nm) included in Tl X. No fluorescence is seen in phenanthrene, chrysene, and pyrene under these conditions.

phenylene and coronene do not pass through the window (~8 Å) to reach the supercage. This is consistent with the report that the largest molecule admitted into a faujasite supercage is decahydrochrysene,[10] a molecule of dimensions slightly less than those of triphenylene and coronene. It is also important to note that the heavy-cation effect in zeolites is general, and room temperature phosphorescence can be observed with a large number of aromatics if they are small enough to pass through the window of the supercage. In Figure 7, the room temperature emission spectra for several aromatics in Tl X are given. In all cases except anthracene, only phosphorescence is observed. With anthracene, both fluorescence and phosphorescence are seen. The smaller heavy-atom effect observed with anthracene is consistent with its short singlet lifetime.[11] Cation-dependent singlet lifetimes and P/F ratios for several aromatics are provided in Table II. The trend in the variation of these two parameters with cation seen in Table II is closely similar to that observed for naphthalene (Table I).

The importance of the heavy-atom cation in inducing significant phosphorescence is also confirmed by the photophysical behavior of various aromatics included in partially cesium exchanged Na X. In Table III the P/F ratios for several aromatics in [Na, Cs] X are provided. The ratio of Cs^+ to Na^+ has a profound influence on the P/F ratio. An exponential relationship observed between Cs^+/Na^+ and P/F has been noted earlier in micellar systems.[12]

It is evident from the data provided here that the cation effect observed in zeolites is general, and thallium-exchanged zeolites can serve as a matrix in which to observe triplet emission at room

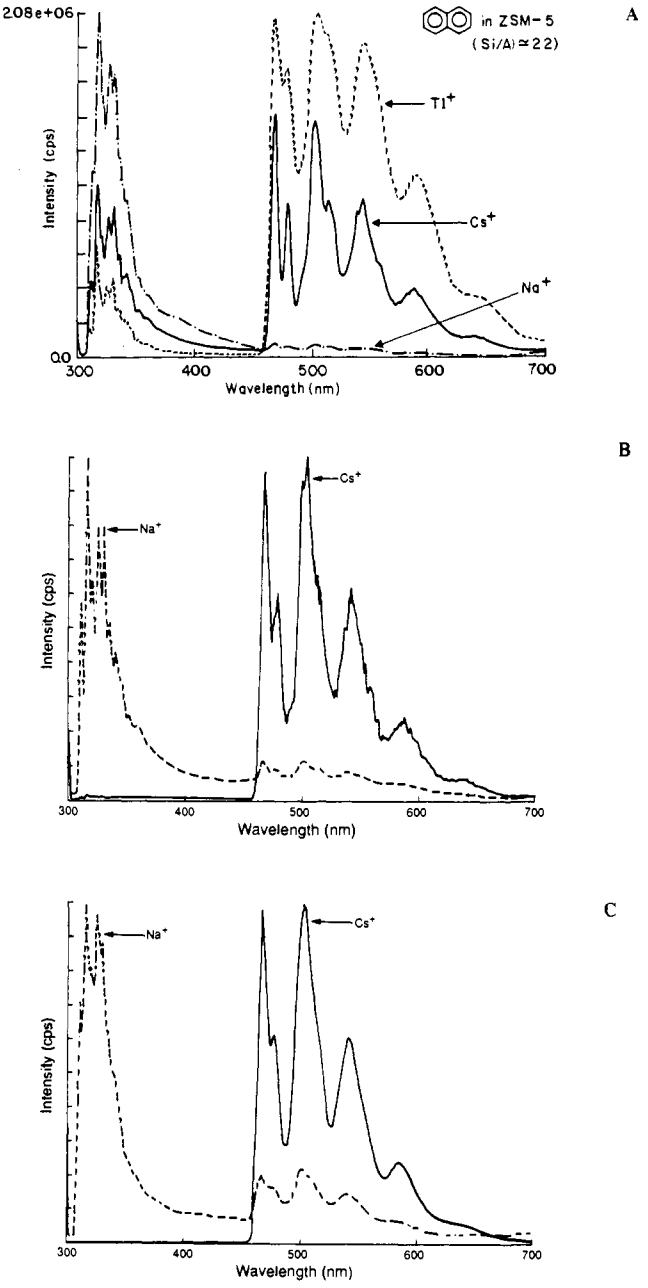

Figure 8. Emission spectra at 298 K of naphthalene (A) in ZSM-5 (Na, Cs, and Tl): (B) in mordenite (Na and Cs); and (C) in β (Na and Cs) (excitation λ in all cases: 285 nm).

temperature. It should also be noted that the effect is not restricted to faujasites alone. It is general in terms of zeolites. Cation-dependent emission of naphthalene included in ZSM-5, mordenite, and β illustrated in Figure 8 supports this claim. Workers should be cautioned that thallium-exchanged zeolites show inherent strong emission in the region 300–500 nm upon excitation in the region ~250–300 nm (the emission originates from Tl^+).

(10) Dyer, A. *Zeolite Molecular Sieves*; John Wiley: New York, 1988; p 95.
(11) Murov, S. L. *Handbook of Photochemistry*; Marcel Dekker: New York, 1973; p 3.
(12) Humphry-Baker, R.; Moroi, Y.; Gratzel, M. *Chem. Phys. Lett.* **1978**, *58*, 207. Kalyanasundaram, K.; Grieser, F.; Thomas, J. K. *Chem. Phys. Lett.* **1977**, *51*, 501. Cline Love, L. J.; Weinberger, R.; Yarmchuk, P. In *Surfactants in Solution*; Mittal, K. L., Lindman, B., Eds.; Plenum: New York, 1984; Vol. 2, p 1139.

Table III. Phosphorescence to Fluorescence Emission Intensity Ratio[a] for Aromatics Included in [Na, Cs] X Zeolites (Percentage of Cs^+ Varied)[b]

[Na, Cs] X Cs:Na ratio[c]	naphthalene	phenanthrene	chrysene	hexahydro-pyrene
0.025	0.15	0.9	1.6	0.4
0.08	1.2	4.7	4.8	0.6
0.14	2.2	6.3	17.6	0.9
0.19	4.3	10.6	31.5	1.4
0.39	6.3	23.8	50.1	2.6

[a] Phosphorescence to fluorescence intensity ratio estimated at 77 K; the number is independent of the wavelength of excitation. [b] Loading level in all cases corresponds to about 0.01. [c] Na X has been exchanged with Cs^+ ion to different levels. The ratio of Cs^+ to Na^+ ions was determined by elemental analyses.

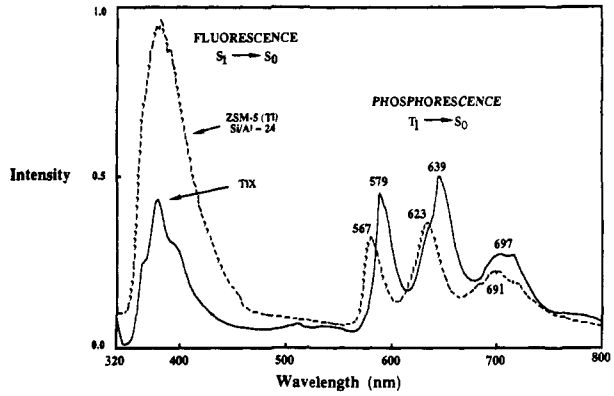

Figure 9. Emission spectra at 298 K of *trans*-stilbene included in Tl X and in Tl ZSM-5 (excitation λ: 290 nm; Corning glass filter 0–51 is used to cut off the second order). Note the intense phosphorescence in both cases.

2. Olefins. Given the success of the zeolite matrices in enabling direct detection of aromatic organic triplets, and the demonstration that the effect originates in the formation of weak cation–chromophore π-complexes,[13] we expanded upon the types of chromophores which can be observed. Medium-enhanced room temperature phosphorescence has attracted considerable attention during the last decade.[14] Several media (filter paper, silica gel, cyclodextrin, solid sodium acetate, and various polymers and micelles) have been used in this context. All of these studies are restricted to the detection of phosphorescence from aromatics and heterocyclics. We show below that, with the use of zeolites as the medium, one can detect phosphorescence from systems which have traditionally escaped detection.

A. Phosphorescence from Stilbenes. Excitation of *trans*-stilbene included in Tl X and in Tl ZSM-5 produces phosphorescence and fluorescence emissions both at room temperature and at 77 K (Figure 9). The temperature has little influence on the ratio of phosphorescence to fluorescence intensities at least in the range 77–300 K (P/F at room temperature, 0.83; at 77 K, 0.63). Emission in the region 550–750 nm having a submillisecond lifetime (0.50 ± 0.08 ms in Tl ZSM-5 and 0.28 ± 0.065 ms in Tl X at 77 K) is quenched by oxygen both at 77 K and at room temperature. A comparison of the ratio P/F in the presence and in the absence of oxygen at room temperature and at 77 K (P/F at room temperature, absence of oxygen 0.83, presence of oxygen 0.02; at 77 K, absence of oxygen 0.63, presence of oxygen 0.09) reveals that the efficiency of oxygen quenching under the same oxygen pressure is much higher at room temperature than at 77 K. This is consistent with the general observation that the translational mobility of molecules within zeolite channels and cavities is inversely related to temperature.[15] The triplet emission

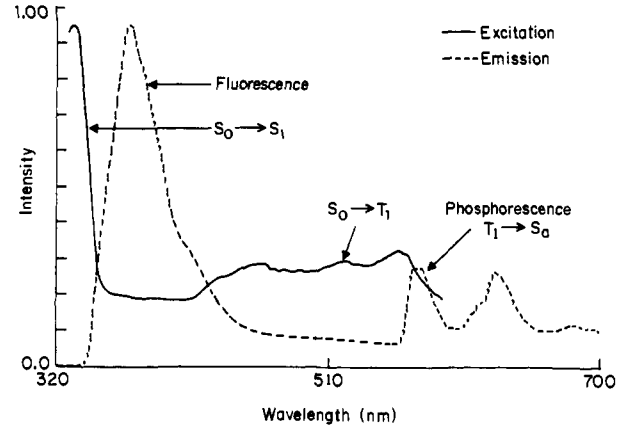

Figure 10. Phosphorescence excitation spectra at 77 K of *trans*-stilbene included in Tl X (emission monitored at 570 nm). Note the presence of an S_0 to T_1 transition. Emission spectrum is also shown for comparison.

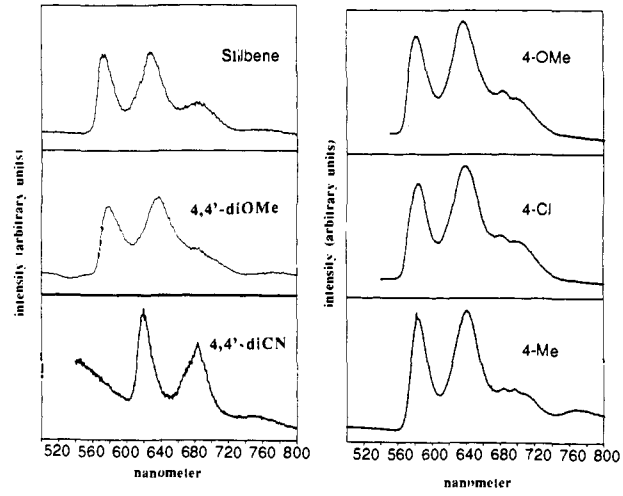

Figure 11. Phosphorescence spectra at 77 K of para-substituted *trans*-stilbene (stilbene; 4,4′-dimethoxy; 4,4′-dicyano; 4-methoxy; 4-chloro; 4-methyl) included in Tl X. Excitation λ in all cases: 320 nm. For spectral band maxima see Table IV.

band positions observed in Figure 9 are in the same region reported earlier for phosphorescence.[16] More importantly, the excitation spectra consist of both S_0 to S_1 and S_0 to T_1 transitions (Figure 10), the latter being in the same region recorded by the oxygen perturbation technique.[17] These factors strongly indicate that the long-wavelength emission is indeed phosphorescence. In addition to *trans*-stilbene, we have recorded phosphorescence at 77 K and at room temperature from a number of substituted *trans*-stilbenes (Chart II). The triplet emission spectra at 77 K for substituted stilbenes included in Tl X are provided in Figure 11. The emission maxima for these in Tl X and in Tl ZSM-5 along with the literature values in organic glass at 77 K are given in Table IV. The triplet emission maxima measured in the present study agree well with the literature reports.[18] The ability to record phosphorescence from stilbenes, even at room temperature, is significant as only very weak phosphorescence from *trans*-stilbene and several substituted *trans*-stilbenes has been recorded at 77 K in organic glass containing ethyl iodide as the heavy atom perturber.[16,18]

B. Phosphorescence from 1-Phenylcycloalkenes and Acyclic Phenylalkenes. In an effort to expand the utility of these zeolite hosts for the observation of phosphorescence from triplet states

(13) Ramamurthy, V.; Caspar, J. V.; Corbin, D. R.; Schlyer, B. D.; Maki, A. *J. Phys. Chem.* **1990**, *94*, 3391.

(14) Vo-Dinh, T. *Room Temperature Phosphorimetry in Chemical Analysis*; John Wiley: New York, 1984. Hurtubise, R. *Phosphorimetry*; VCH: New York, 1990.

(15) Post, H. F. M. In *Introduction to Zeolite Science and Practice*; van Bekkum, H., Flanigen, E. M., Jansen, J. C., Eds.; Elsevier: Amsterdam, 1991; p 392.

(16) Saltiel, J.; Khalil, G. E.; Schanze, K. *Chem. Phys. Lett.* **1980**, *70*, 233.

(17) Evans, D. F. *J. Chem. Soc.* **1957**, 1351. Dyck, R. H.; McClure, D. S. *J. Chem. Phys.* **1962**, *36*, 2326.

(18) Gorner, H. *J. Phys. Chem.* **1989**, *93*, 1826.

Table IV. Zeolite-Dependent Triplet Emission Band Maxima (nm)[a] of *trans*-Stilbenes and *all-trans*-1,4-Diarylbutadienes

olefin	Tl X	Tl ZSM-5	EPA glass[b]
phenylindene	566, 620, 678	553, 605, 659	567, 620, 680
indenoindene	542, 591, 648	548, 597, 654	548, 595, 652
stilbene	579, 639, 697	567, 623, 691	578, 635, 700
4,4′-dimethoxystilbene	592, 650	577, 636	590, 645
4,4′-dicyanostilbene	617, 685	620, 684	622, 680
4-methylstilbene	587, 645, 703	583, 640, 701	–
4-methoxystilbene	590, 649, 702	581, 636, 699	592, 646
4-(methoxycarbonyl)stilbene	602, 663, 723	590, 649, 706	–
4-chlorostilbene	588, 647, 706	583, 638, 700	591, 645
1,4-diphenylbutadiene	698, 780	686, 765	–
1-(*p*-chlorophenyl)-4-phenylbutadiene	698, 786	698, 784	–
1-(*p*-methylphenyl)-4-phenylbutadiene	706, 793	692, 778	–
1-(*p*-methoxyphenyl)-4-phenylbutadiene	703, 791	699, 786	–
1-[*p*-(methoxycarbonyl)phenyl]-4-phenylbutadiene	709, 806	710, 808	–
1,4-bis(*p*-cyanophenyl)butadiene	738, 818	740, 820	–

[a] Band maxima based on emission spectra recorded at 77 K and corresponding to the major emission. See text for excitation wavelength dependence on the emission maxima in Tl X. [b] Literature values from the following: Saltiel, J.; Khalil, G. E.; Schanze, K. *Chem. Phys. Lett.* **1980**, *70*, 233. Gorner, H. *J. Phys. Chem.* **1989**, *93*, 1826. Phosphorescence spectra recorded in organic glass containing ethyl iodide.

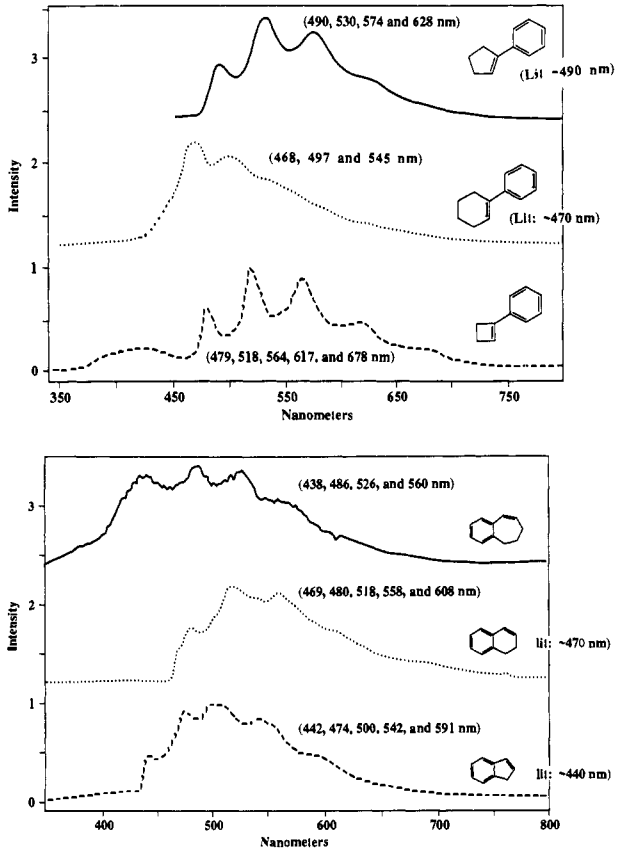

Figure 12. Phosphorescence spectra at 77 K for 1-phenylcycloalkenes (A) and phenyl-fused cycloalkenes (B) included in Tl X. Excitation wavelength shown on the figure. For triplet energies based on the above spectra and comparison with the literature values, see Table V.

which have not heretofore been observable, we have investigated the photophysics of several 1-phenylcycloalkenes and acyclic phenylalkenes (Chart II) included in thallium-exchanged zeolites. Triplet emission from cyclic or acyclic phenylalkenes has not been observed before. The triplet energies of these systems are generally obtained from the oxygen-enhanced and heavy-atom-perturbed S_0 to T_1 absorption spectra.[19] In Figure 12 the triplet emission spectra at 77 K of several 1-phenylcycloalkenes and acyclic phenylalkenes included in Tl X are provided. Similar spectra were recorded in Tl Y and in Tl ZSM-5. For compounds for which literature estimates are available, the 0–0 transition of the

(19) Ni, T. N.; Caldwell, R. A.; Melton, L. A. *J. Am. Chem. Soc.* **1989**, *111*, 457. Crosby, P. M.; Dyke, J. M.; Metcalfe, J.; Rest, A. J.; Salisbury, K.; Sodeau, J. R. *J. Chem. Soc., Perkin Trans. 2* **1977**, 182.

Table V. Singlet–Triplet Energy Gaps ($\Delta_{T_1 \rightarrow S_0}$) for All-Trans α,ω-Diphenyl Polyenes and Simple Olefins Included in Tl X Zeolite[a]

polyene	λ_{0-0} $T_1 \rightarrow S_0$ (nm)	λ_{0-0} $S_0 \rightarrow T_1$ (nm)
trans-stilbene	579	563
1,4-diphenyl-1,3-butadiene	698	680
1,6-diphenyl-1,3,5-hexatriene	818	830
1,8-diphenyl-1,3,5,7-octatetraene	924	890, ≈990
1-phenylcyclopentene	490	490
1-phenylcyclohexene	468	470
indene	442	440
1,2-dihydronaphthalene	469	470

[a] As determined from the position of the 0–0 band of phosphorescence spectra (λ_{0-0}) at 77 K. Literature estimates of $\Delta_{T_1 \rightarrow S_0}$ from absorption spectra ($S_0 \rightarrow T_1$) and energy-transfer studies are included for comparison. Literature values from the following: Ni, T. N.; Caldwell, R. A.; Melton, L. A. *J. Am. Chem. Soc.* **1989**, *111*, 457. Crosby, P. M.; Dyke, J. M.; Metcalfe, J.; Rest, A. J.; Salisbury, K.; Sodeau, J. R. *J. Chem. Soc., Perkin Trans. 2* **1977**, 182. Heinrich, G.; Holzer, G.; Blume, H.; Schulte-Frohlinde, D. *Z. Naturforsch.* **1970**, *25B*, 496; Evans, D. F.; Tucker, J. N. *J. Chem. Soc., Faraday Trans. 2* **1972**, *68*, 174.

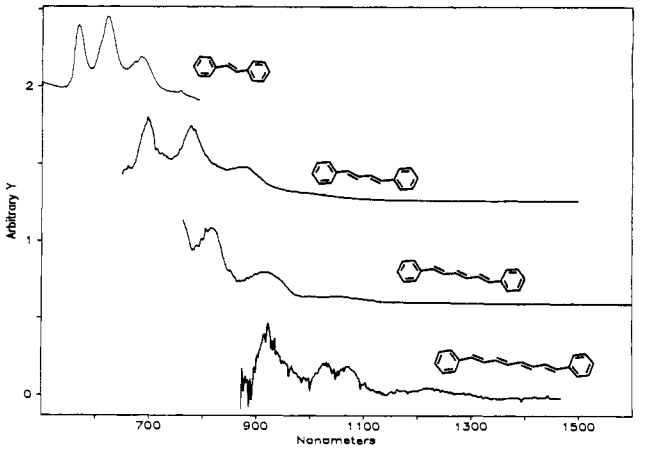

Figure 13. Phosphorescence spectra at 77 K of α,ω-diphenyl polyenes included in Tl X. Excitation λ: stilbene, 295 nm; diphenylbutadiene, 340 nm; diphenylhexatriene, 350 nm; diphenyloctatetraene, 375 nm. For triplet energies based on the above spectra and comparison with the literature values, see Table V.

phosphorescence emission and the reported S_0 to T_1 absorption agree remarkably well (Table V), providing confidence in our technique as well as in the oxygen-enhanced and heavy-atom-perturbed absorption techniques.[19]

C. Phosphorescence from α,ω-Diphenyl Polyenes. All-trans α,ω-diphenyl polyenes exhibit very low intersystem-crossing efficiencies and efficient fluorescence and are expected to phos-

Chart II

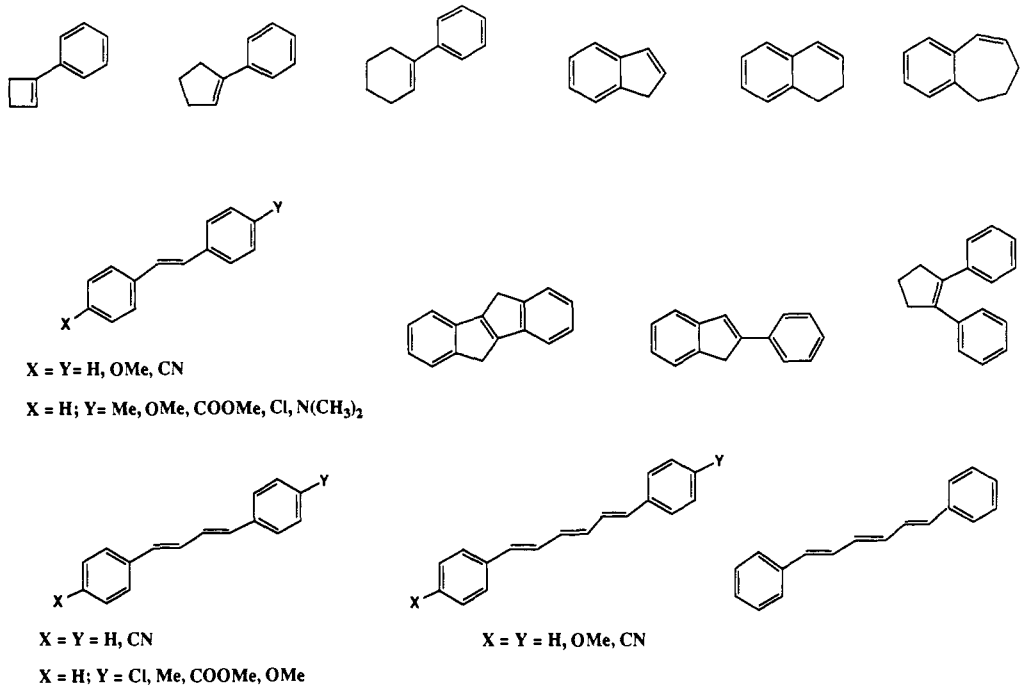

phoresce at low energies where detection with conventional photomultipliers is impractical.[20] To our knowledge, no authentic phosphorescence spectra from these have been reported. Our approach to this problem has been to combine the use of the zeolite hosts and their prodigious heavy-atom effects with the use of a sensitive germanium detector to enable the detection of the phosphorescence of the α,ω-diphenyl polyenes. Figure 13 shows the observed phosphorescence of the α,ω-diphenyl polyenes included in Tl X. At 77 K, we observed a well-resolved structured emission for each of the polyenes, with a prominent vibronic spacing of 1200–1400 cm^{-1}, as expected for triplet phosphorescence. The singlet–triplet energy gaps ($\Delta_{T_1 \rightarrow S_0}$) obtained from the observed 0–0 lines (Table V) are in excellent agreement with literature predictions from $S_0 \rightarrow T_1$ absorption spectra obtained by the O_2 perturbation method and from energy-transfer studies.[21] The phosphorescence emission maxima recorded for a number of 1-(*p*-substituted phenyl)-4-phenylbutadienes are summarized in Table IV. We believe that this is the first unambiguous observation of triplet phosphorescence from any of these diphenyl polyenes.

D. Wavelength-Dependent Triplet Emission. Emission spectra are independent of the wavelength of excitation for all the olefins included in Tl ZSM-5. However, the emission maxima were dependent on the excitation wavelength for several olefins when included in either Tl X or in Tl Y. This was very pronounced for stilbenes and was independent of the temperature in the range 3.4–300 K. A minor emission with maxima slightly different from the major emission was observed upon excitation on the tail of the absorption spectra of several of the olefins. As an example, emission spectra of *trans*-stilbene in Tl X at 3.4 K at three different excitation wavelengths are provided in Figure 14. It is important to note that the emission spectra changed significantly with a small variation in the excitation wavelength (340–344 nm). Careful scanning between 340 and 344 nm gave rise to emission spectra which are a combination of the various percentages of the two displayed for 340 and 344 nm in Figure 14. The excitation spectra recorded for the two emissions are very similar. However, the

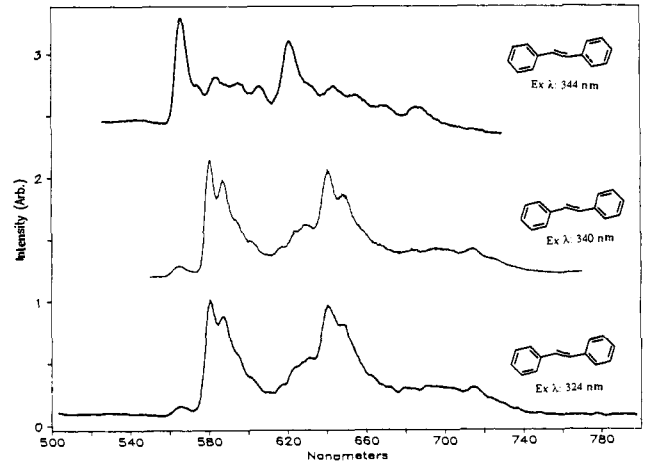

Figure 14. Excitation wavelength dependent phosphorescence spectra at 4 K of *trans*-stilbene included in Tl X. Excitation wavelength indicated on the spectrum.

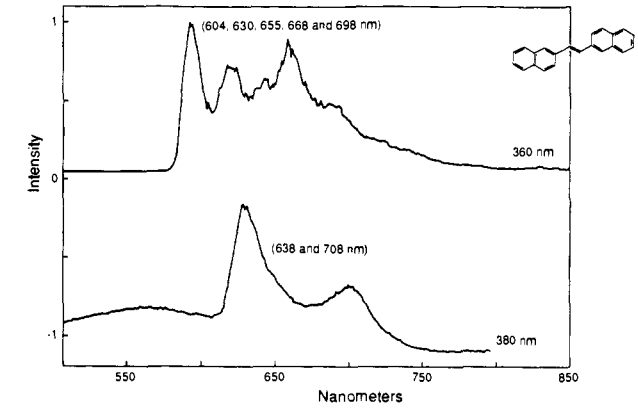

Figure 15. Excitation wavelength dependent phosphorescence spectra at 77 K of *trans*-1,2-dinaphthylethylene included in Tl X. Excitation wavelength indicated on the spectrum.

lifetimes at 10 K of the two emissions monitored at 566 and 580 nm were slightly different (5.67 ± 0.08 ms and 4.21 ± 0.07 ms). Another example, 1,2-dinaphthylethylene, displayed in Figure 15, also shows wavelength-dependent emission (360 vs 380 nm). These

(20) Görner, H. *J. Photochem.* **1982**, *19*, 343. Hudson, B.; Kohler, B. *Annu. Rev. Phys. Chem.* **1974**, *25*, 437. Bensasson, R.; Land, E. J.; Lafferty, J.; Sinclair, R. S.; Truscott, T. G. *Chem. Phys. Lett.* **1976**, *41*, 333. Allen, M. T.; Whitten, D. G. *Chem. Rev.* **1989**, *89*, 1691.

(21) Heinrich, G.; Holzer, G.; Blume, H.; Schulte-Frohlinde, D. *Z. Naturforsch.* **1970**, *25B*, 496. Evans, D. F.; Tucker, J. N. *J. Chem. Soc., Faraday Trans. 1* **1972**, *68*, 174.

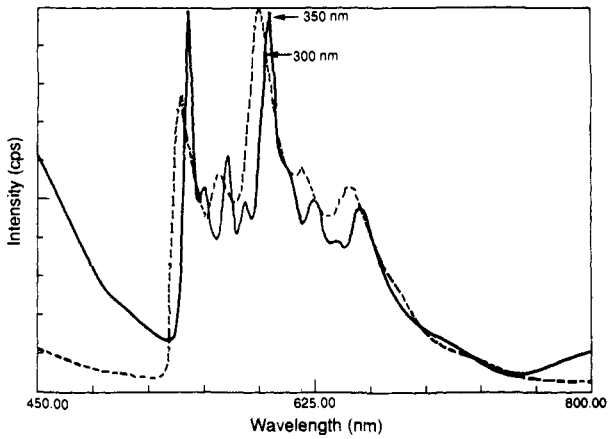

Figure 16. Excitation wavelength dependent phosphorescence spectra at 77 K of indenoindene included in Tl X. Excitation wavelength indicated on the spectrum.

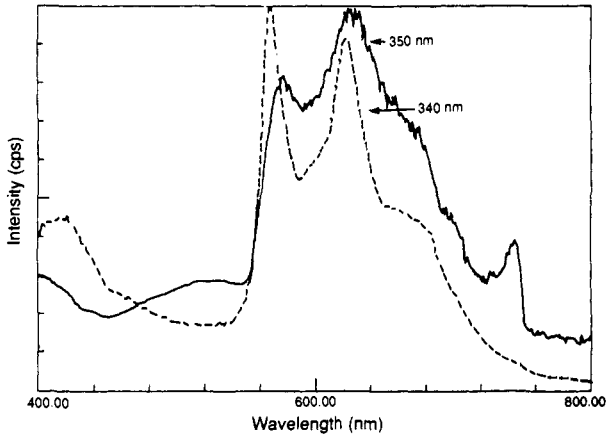

Figure 17. Excitation wavelength dependent phosphorescence spectra at 77 K of phenylindene included in Tl X. Excitation wavelength indicated on the spectrum.

observations suggest that not all molecules of the guest included within X and Y zeolites reside in identical environments. We are unable to conclude whether such a difference is due to the presence of various conformers or due to the presence of nonidentical sites within the supercages of X and Y zeolites. Our dilemma is further complicated by the behavior of phenylindene and indenoindene, rigid analogues of *trans*-stilbene. These, as illustrated in Figures 16 and 17, also show wavelength dependence. Indenoindene, which has only one conformer, shows a small wavelength dependence, suggesting that the cause of wavelength dependence might be the presence of nonidentical sites. On the basis of model compounds, while the two emission spectra observed for *trans*-stilbene can be ascribed to two conformers (see next section for further discussion), the two emissions seen in the case of phenylindene cannot be. Clearly, further work is required to answer the question, is the wavelength dependence due to the presence of different conformers or due to guests present in different sites?

E. Zeolite-Dependent Triplet Emission. The triplet emissions observed for a number of stilbenes and a few 1,4-diarylbutadienes included in Tl ZSM-5 are consistently blue-shifted with respect to the emission reported in glassy matrices and that in Tl X (Table IV). Our initial belief that conformation may play an important role in this phenomenon was supported by the fact that the emission maxima for indenoindene, which has no conformational isomers, are the same both in a glassy matrix and in Tl ZSM-5. A comparison of the maxima for *trans*-stilbene with those of the rigid analogues of *trans*-stilbene, phenylindene and indenoindene, revealed to us that conformations of *trans*-stilbene included in Tl ZSM-5 are different from the one observed in a glassy matrix. On the basis of the model compounds shown in Chart III, one can conclude that, in *trans*-stilbene, coplanarity of the phenyl ring(s) with the central olefinic bond may determine the phosphorescence λ_{max}; maxima are at the shortest wavelength when both the rings are planar and at the longest wavelength when both are twisted with respect to the central bond. An equivalent conformation of *trans*-stilbene analogous to the rigid model compounds is also shown in Chart III. On the basis of this comparison, one can conclude that when *trans*-stilbene enters the channels of ZSM-5, it is preferentially included in a conformation in which one of the phenyl rings is planar with respect to the central bond while the other is partially twisted. Similarly, when phenylindene enters the channel, it probably attains a better planarity than is present in solution.

Chart III

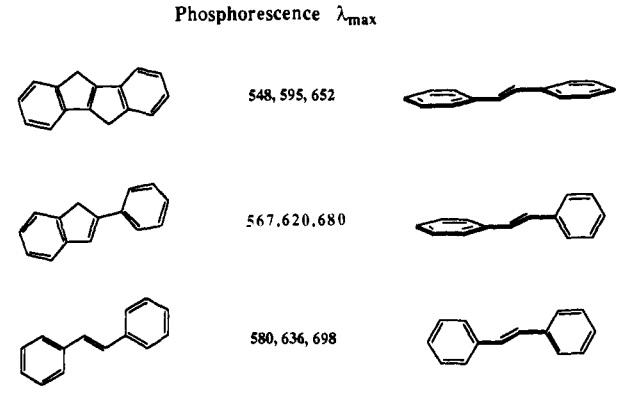

F. Limitations. In spite of our success in monitoring the phosphorescence from a large number of olefins at room temperature, we were unable to record triplet emission from any systems not containing phenyl substitution (retinyl polyenes, simple alkyl dienes, alkyl trienes, etc.). Even with the phenyl substitution, we were unable to record triplet emission from simple styrenes and related derivatives. Another system which escaped our technique is *cis*-stilbene and the rigid *cis*-stilbene model compound 1,2-diphenyl-1-cyclopentene. It is also important to note that we were not able to detect any phosphorescence from any of the systems described in Chart II when rubidium or cesium was the cation. The presence of thallium ion seems to be very critical. Also, it is to be noted that we cannot detect any emission when mechanical mixtures of thallium nitrate and the olefins are excited, indicating the importance of the zeolite matrix.

3. Heavy-Atom Effect as a Tool To Understand Zeolite–Guest Interaction. A. Inter- and Intracrystalline Migration of Molecules Included in Zeolites. Knowledge of diffusional motions of molecules between crystallites and within the same crystallite are of considerable importance in predicting the influence of zeolites on the photobehavior of included guest molecules. Monitoring the cation-dependent phosphorescence to fluorescence ratio allows for easy investigation of molecular migration of aromatic guest molecules between zeolites having different cations. For example, the emission of the Na X–naphthalene complex consists essentially only of fluorescence. If this complex is mixed with Cs X, then any physical migration of naphthalene from Na X to Cs X should be detectable as a change in the phosphorescence to fluorescence intensity ratio. The P/F ratio can provide information concerning the extent of migration. In order to answer the basic question, does a guest molecule migrate from one crystallite to another, an aromatic–zeolite complex and an empty dry zeolite were mixed together in three different ways, and the progress of the migration was followed by monitoring the emission spectra of the solid mixture: (a) Dry zeolite–aromatic complex and dry empty zeolite (having different anions) were kept in a sealed vial; (b) dry zeolite–aromatic complex and dry empty zeolite (having different cations) were ground together and kept in a sealed vial; and (c) dry zeolite–aromatic complex and dry empty zeolite (having different cations) were kept in a sealed glass tube separated by glass wool. Spectra of the mixture or of the two portions in the last case were recorded periodically over 5 days. Naphthalene, phenanthrene, and chrysene were used as guests. The host combinations consisted of Cs X–Na X, Na X–Cs X, Cs Y–Na Y, and

Na Y–Cs Y (in all cases the former zeolite is the one with which the aromatic is originally complexed and the latter is the empty one). In none of these cases did we see any change in the emission spectra, indicating that no migration of the guest from one zeolite to the other occurred. This suggests that the guest molecules are tightly held within the supercages of the original zeolite at room temperature. It is, however, important to note that such migrations are promoted in the presence of a solvent such as trimethylpentane or hexane. The above mixtures of empty and guest-filled zeolites were stirred in hexane or trimethylpentane, and the solid complexes were collected and dried. The emission spectra of the above dry, solvent-free complexes prepared after stirring with solvent indicated that the guest molecules have distributed themselves between the two zeolites. Thus, it is clear that, while in the absence of a solvent, guest molecules do not migrate from one solid zeolite to the other, they do so in the presence of a solvent (zeolite–solvent slurry).

Our results also provide the background for a new approach for monitoring diffusion of organic guests inside zeolites (intracrystalline). Preparation of zeolite samples containing mixtures of more than one cation (e.g., containing both Na^+ and Cs^+ to different levels) such that the majority of supercages contain only the lighter cations should yield phosphorescence lifetimes which are biexponential under conditions where the adsorbed naphthalene cannot diffuse between cages within the excited-state lifetime. As the temperature is increased and diffusion begins to allow the naphthalene triplet to encounter the heavier cation prior to decay, the phosphorescence kinetics will begin to change until temperatures are reached where diffusion becomes rapid on the excited-state time scale. The phosphorescence lifetime will then become monoexponential with a value typical for a zeolite sample containing only the heavier cation. In principle, this approach can be used as well for monitoring singlet lifetimes. The power of the technique derives from both the sensitivity to local environment and the range of time scales accessible, ranging from nanoseconds for singlet states up to seconds for triplets. In preliminary studies of this type, we have found that for phenanthrene included in [Na,Cs] X zeolites where the Cs^+ content is low (0.5%), the triplet lifetime at 77 K is biexponential and the two observed lifetimes (0.26 and 2.0 s) are identical to those observed for phenanthrene included in pure Cs X and Na X, respectively. When the Cs^+ content is increased (4%), the 77 K lifetimes become monoexponential with a value of 0.27 s, indicating that all excited states are contacting Cs^+. We believe that, at both lower and higher Cs^+ loading levels, phenanthrene molecules migrate within the zeolite crystallite. At higher levels of Cs^+, the diffusing molecules apparently find a Cs ion before they decay from the triplet. Variable-temperature studies and detailed analyses of these effects are needed to quantitatively understand this process.

B. Partitioning of Guests between Two Zeolites. Interaction between the guest aromatic molecules and the zeolite supercage is at least partially controlled by the cation. Interaction, or binding strength, is expected to decrease in the order $Li^+ > Na^+ > K^+ > Rb^+$ and Cs^+.[22] If an equal opportunity is provided to a guest to complex with Li X and Cs X, which one would it prefer? On the basis of the binding energy alone, preferential complexation with Li X would be expected. This is easily tested by the emission technique discussed above. A known amount of aromatic guest (naphthalene, phenanthrene, and chrysene) and equal amounts of two empty dry zeolites ([Li X and Cs X]; [Na X and Cs X]; [K X and Cs X]) were stirred together in hexane or trimethylpentane. After several hours of stirring, the dry complex was collected and the emission spectra were recorded. The P/F ratio in all three mixtures of zeolites was in between that expected for individual complexes of Cs X and Li, Na, or K X, indicating that the guest did not show any preference for the cation. This points out that, in the presence of a solvent, the nature of the cation does not control the complexation behavior. The driving force for guest inclusion in faujasites is most likely the higher polarity of the zeolite interior[23] with respect to outside hexane. The micropolarity of the supercage, even in the presence of hexane, is shown to depend on the cation.[23] It is not clear why naphthalene did not show any preference for the cation. At this stage we provide an easy technique by which one can monitor and understand the process of guest inclusion within zeolites.

(22) Hepp, M.; Ramamurthy, V.; Corbin, D. R.; Dybowoski, C. *J. Phys. Chem.*, in press.

Conclusion

We have demonstrated that heavy atom cation exchanged faujasite zeolites are a versatile new medium for the observation of external-heavy-atom perturbation of organic triplet excited states. The large magnitude of the external-heavy-atom perturbation is not unique to the X-type faujasites; we have observed similar effects for organic guests included in Y-type faujasites, in pentasils, and in others. Heavy-atom-induced changes in the photophysical properties of the guest are also a useful tool to probe the various physical phenomena that occur during guest–zeolite interaction. Present results clearly attest to the vast and untapped potential of zeolites as microenvironments to modify the photochemical and photophysical behavior of organic molecules.

Experimental Section

Zeolites. Zeolites 13X (Na X), LZ-Y52 (Na Y), Na-mordenite and Na-Ω were obtained from Linde. The cation of interest (Li, K, Rb, Cs, and Tl) was exchanged into these powders by contacting the material with the appropriate nitrate solution at 90 °C. For each gram of zeolite, 10 mL of a 10% nitrate solution was used. This was repeated a number of times. The samples were then thoroughly washed with water and dried. Exchange loadings were typically between 37 and 84%. Samples of Na TPA-ZSM-5 with the Si/Al ratio varying from 20 to 550 were prepared by a slight modification of Rollman and Volyocsik's procedure.[24] Samples were calcined in flowing air at 60 °C/h to 550 °C and then held at 550 °C for 10 h to give Na ZSM-5. The samples were then exchanged by the method described above to give Li ZSM-5, K ZSM-5, Rb ZSM-5, Cs ZSM-5, and Tl ZSM-5. Samples of Na-β were prepared by literature methods,[25] calcined in flowing air at 60 °C/h to 550 °C, and then held at 550 °C for 10 h to give Na-β. The samples were then exchanged by the method described above to give Rb-β, Cs-β and Tl-β. All samples were subjected to elemental analysis. The exchange level of the cation was above 70%. These samples were stored under ambient conditions. Samples having a Si/Al ratio of 22 were used for emission studies.

Activation of Zeolites. Zeolites were activated as follows. In general, ca. 250 mg of zeolite was placed in a silica crucible and heated at 500 °C for about 12 h. The freshly activated zeolites were rapidly cooled in air to ca. 50 °C and added to solutions of the guests of interest. Activated zeolites were used immediately after activation. In general, we have found that the time required for these activated zeolites to readsorb water to their full capacity is about 10 h under our laboratory conditions, and of course this varies with the zeolites. The rehydration is easily monitored by keeping the activated zeolites on the pan of an analytical balance and watching the weight change.

Organic Guests. Aromatic guests and α,ω-diphenyl polyenes were commercial samples (Aldrich or Fluka) and were recrystallized at least four times prior to use. Substituted stilbenes and dienes were synthesized by conventional procedures and were purified by several recrystallizations. The indenoindene and dinaphthylethylene samples were kindly provided by J. Saltiel, and the rest of the olefins were kindly supplied by R. S. H. Liu and A. Asato. These were used as received.

Preparation of Zeolite Complexes. A. Solution Method. Known amounts of aromatics or olefins and the activated zeolites were stirred together in 20 mL of hexane (in the case of X, Y, mordenite, β, and Ω zeolites) or trimethylpentane (ZSM zeolites) for about 10 h. In a typical preparation, 250 mg of the zeolite and 0.01 mg of the guest were taken in 20 mL of the solvent. White or lightly colored powder, collected by filtration of the solvent, was washed with dry hexane several times and dried under nitrogen. Samples were taken in Pyrex cells fitted with Teflon stopcocks, degassed thoroughly (10^{-5} mm), and sealed.

B. Solid Method. Known amounts of the aromatic/olefin and the zeolite were taken in a mortar and were mixed well under a nitrogen atmosphere. The mixture, in an ESR tube, was sealed and annealed for

(23) Ramamurthy, V.; Sanderson, D. R.; Eaton, D. F. *Photochem. Photobiol.*, in press. Ramamurthy, V.; Caspar, J. V. *Mol. Cryst. Liq. Cryst.* **1992**, *211*, 211.

(24) Rollman, L. S.; Volyocsik, E. K. In *Inorganic Syntheses*; Wiley: New York, 1983; pp 61–68.

(25) Wadlinger, R. L.; Kerr, G. T.; Rosinski, E. J. U.S. Patent No. 3,308,069, 1975, Example 7.

24 h at 50 °C to ensure an equilibrium distribution of guest molecules in the zeolite.

C. **Diffuse Reflectance Spectra.** Diffuse reflectance spectra of the zeolite solid samples were measured in 2-mm-path-length quartz cells using a Varian 2400 spectrometer equipped with either an integrating sphere (Varian) or a "praying mantis" all reflective light collection system (Harrick Scientific), in both cases using barium sulfate (Kodak, white reflectance standard) as the reference. Sample packing densities were not determined nor were they specifically controlled. Spectra were recorded between 220 and 800 nm. For comparison, spectra of the empty zeolites were also recorded. Data were recorded digitally, and appropriate background corrections were carried out using the computer program SpectraCalc (Galactic Industries).

D. **Emission Spectra.** Emission spectra were recorded at room temperature and at 77 K in Supracil quartz EPR tubes under degassed conditions with a Spex Fluorolog 212 or 222 spectrofluorimeter. Spectra were corrected for detector sensitivity. Near-IR emission spectra from long-chain polyenes were recorded using a Spex 212 fluorimeter (Spex Industries) modified to accept a high-sensitivity germanium detector (North Coast Model EO-817L, useful wavelength range ≈750–1750 nm). Spectra were corrected for detector and optical system response using curves determined with an NBS-traceable, calibrated tungsten lamp (Optronics Laboratories). The signal to noise ratio was improved by lock-in detection (Stanford Instruments) with the chopper located at the entrance slit of the emission monochromator. Scattered light was removed by use of either short-wave-pass or narrow-band-pass interference filters (Corion Corp.) placed between the excitation monochromator and the sample and by use of long-wave-pass interference filters (Corion Corp.) placed between the sample and the emission monochromator. Background scans of both as prepared and activated zeolite samples showed no detectable emission in this wavelength region.

E. **Lifetimes.** Fluorescence lifetimes were measured at room temperature using a PRA single photon counting apparatus, deconvolution was performed by nonlinear least-squares routines minimizing χ^2, and goodness of fit was determined with plots of residuals, autocorrelation function, and reference to the Durbin-Watson statistic.[26] All decays except that for Cs X could be fitted to a single-exponential function. Triplet lifetimes were measured by conventional flash photolysis techniques using a xenon flash lamp as the excitation source. Emission intensities were monitored at the maximum of the 0–0 vibronic band, and data was fit to simple mono- or biexponential decay laws using an unweighted least-squares analysis.

F. **Oxygen Quenching Studies.** Dry zeolite complex was taken in an ESR tube fitted with a Teflon stopcock and degassed thoroughly (10^{-5} mm) on a vacuum line fitted with double-valved stopcocks for oxygen and nitrogen leaks. The degassed sample was filled with oxygen at high pressures. The degassing and oxygen-filling cycle was repeated three times. The spectrum of the sample thus filled with oxygen was recorded. In all cases, after the emission spectrum was recorded, the sample was either filled with nitrogen or degassed thoroughly. The intensities of the fluorescence and phosphorescence reached the original levels before oxygen filling. The oxygen and nitrogen cycle was carried out at least three times, and to our great surprise the intensities of the emissions were highly reproducible.

Acknowledgment. It is a pleasure to thank D. R. Sanderson, A. Pittman, J. Lockhart, and P. Hollins for expert technical assistance. We are thankful to Professors R. S. H. Liu and J. Saltiel and Dr. A. Asato for samples of olefins and useful discussions.

Registry No. (*E*)-4-MeOC$_6$H$_4$CH=CHC$_6$H$_4$-4-OMe, 15638-14-9; (*E*)-4-CNC$_6$H$_4$CH=CHC$_6$H$_4$-4-CN, 5216-37-5; (*E*)-4-MeC$_6$H$_4$CH=CHPh, 1860-17-9; (*E*)-4-MeOC$_6$H$_4$CH=CHPh, 1694-19-5; (*E*)-4-MeOC(O)C$_6$H$_4$CH=CHPh, 1149-18-4; (*E*)-4-ClC$_6$H$_4$CH=CHPh, 1657-50-7; (*E,E*)-PhCH=CHCH=CHPh, 538-81-8; (*E,E*)-4-ClC$_6$H$_4$CH=CHCH=CHPh, 37985-13-0; (*E,E*)-4-MeC$_6$H$_4$CH=CHCH=CHPh, 37985-11-8; (*E,E*)-4-MeOC$_6$H$_4$CH=CHCH=CHPh, 22145-08-0; (*E,E*)-4-MeOC(O)C$_6$H$_4$CH=CHCH=CHPh, 89510-60-1; (*E,E*)-4-CNC$_6$H$_4$CH=CHCH=CHC$_6$H$_4$-4-CN, 89510-54-3; (*E*)-PhCH=CHPh, 103-30-0; (*E,E,E*)-Ph(CH=CH)$_3$Ph, 17329-15-6; (*E,E,E,E*)-Ph(CH=CH)$_4$Ph, 22828-29-1; Li, 7439-93-2; Na, 7440-23-5; K, 7440-09-7; Rb, 7440-17-7; Cs, 7440-46-2; Tl, 7440-28-0; phenanthrene, 85-01-8; pyrene, 129-00-0; hexahydropyrene, 20330-24-9; acenaphthene, 83-32-9; chrysene, 218-01-9; 2-phenylindene, 4505-48-0; indenoindene, 6543-29-9; 1-phenylcyclopentene, 825-54-7; 1-phenylcyclohexene, 771-98-2; indene, 95-13-6; 1,2-dihydronaphthalene, 447-53-0; naphthalene, 91-20-3.

(26) Eaton, D. F. *Pure Appl. Chem.* **1990**, *62*, 1631.

Formation of Carbohydrates in the Reaction of Atomic Carbon with Water

Glenn Flanagan, Sheikh N. Ahmed, and Philip B. Shevlin*

Contribution from the Department of Chemistry, Auburn University, Auburn, Alabama 36849.
Received October 28, 1991

Abstract: The cocondensation of atomic carbon with water at 77 K generates a mixture of straight chain aldoses with up to five carbons. A proposed mechanism involves initial reaction of C with H_2O to give hydroxymethylene which rearranges to formaldehyde. Subsequent nucleophilic addition of hydroxymethylene to formaldehyde with hydrogen transfer generates glycolaldehyde which reacts with additional hydroxymethylenes to build up the higher carbohydrates. Confirmation of this mechanism is provided by deuterium labeling studies.

Atomic carbon has been identified as an interstellar species[1] and in association with cometary emissions.[2] In attempts to determine the reactions which would occur when carbon atoms are condensed on cold surfaces with some of the more abundant extraterrestrial molecules, we have reported that cocondensation of carbon with water and ammonia at 77 K generates amino acids.[3,4] We have now found that low-temperature condensation of carbon with water alone yields carbohydrates.

The initial reaction of atomic carbon with water gives deoxygenation to hydrogen and carbon monoxide along with the divalent carbon intermediate hydroxymethylene, **1**, which can rearrange to formaldehyde as shown in eq 1.[5] We have previously calculated

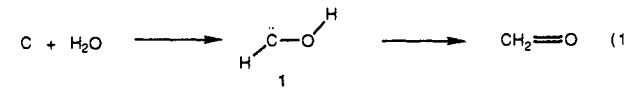

1 (1)

(1) Keene, J.; Blake, G. A.; Phillips, T. G.; Huggins, P. J.; Beichman, C. A. *Astrophys. J.* **1985**, *299* (2, pt. 1), 967.

(2) (a) Balsiger, H. et al. *Nature* **1986**, *321*, 330. (b) Woods, T. N.; Feldman, P. D.; Dymond, K. F. *Astron. Astrophys.* **1987**, *187*, 380, and references cited therein.

(3) Shevlin, P. B.; McPherson, D. W.; Melius, P. *J. Am. Chem. Soc.* **1983**, *105*, 488.

(4) Shevlin, P. N.; McPherson, D. W.; Melius, P. *J. Am. Chem. Soc.* **1981**, *103*, 7006.

(5) Ahmed, S. N.; McKee, M. L.; Shevlin, P. B. *J. Am. Chem. Soc.* **1983**, *105*, 3942.

0002-7863/92/1514-3892$03.00/0